

drawn: (1) Solubility of Np(IV) hydrous oxide under reducing conditions can be used to set upper limits on solubility-controlled concentrations of Np, and these concentrations are below the maximum permissible concentrations in uncontrolled discharge.²⁸ (2) Most carbonate ground waters (<0.01 M total carbonate) will not significantly increase the Np(IV) hydrous oxide solubility

above the maximum permissible concentrations. (3) Contrary to predictions based on thermodynamic data reported in the literature, no evidence was found for amphoteric behavior of Np(IV). (4) The values of tetravalent actinide carbonate complexes reported in the literature are grossly in error.

Acknowledgment. This research was conducted for the U.S. Department of Energy under Contract DE-AC06-76RLO 1830. We thank Margaret McCulloch for analytical assistance.

Registry No. Np, 7439-99-8; NpO₂, 12035-79-9; Na₂S₂O₄, 7775-14-6.

(28) "Standards for Protection Against Radiation", Report 10 CFR 20; U.S. Nuclear Regulatory Commission: Washington, DC, 1979.

Contribution from the Chemistry Departments, Ben-Gurion University of the Negev, and Nuclear Research Centre Negev, Beer-Sheva, Israel

Stabilization of the Monovalent Nickel Complex with 1,4,8,11-Tetraazacyclotetradecane in Aqueous Solutions by N- and C-Methylation. An Electrochemical and Pulse Radiolysis Study

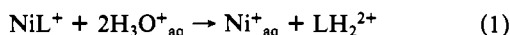
NUSRALLAH JUBRAN,^{1a} GREGORY GINZBURG,^{1a,b} HAIM COHEN,^{*1c} YAACOV KORESH,^{1c} and DAN MEYERSTEIN^{*1a,c}

Received August 11, 1983

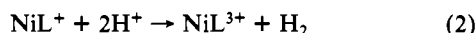
The divalent nickel complexes with 1,4,8,11-tetraazacyclotetradecane (L₁), 1,4,8,11-tetramethyl-1,4,8,11-tetraazacyclotetradecane (L₂), *meso*-5,7,7,12,14,14-hexamethyl-1,4,8,11-tetraazacyclotetradecane (L₃), and 1,4,5,7,7,8,11,12,14,14-decamethyl-1,4,8,11-tetraazacyclotetradecane (L₄) were reduced by reactions with e_{aq}⁻ and CO₂⁻ and by electrochemical reactions in aqueous solutions. The redox potentials of the NiL_i²⁺/NiL_i⁺ couples are -1.58, -1.15, -1.42, and -0.98 V vs. SCE for *i* = 1, 2, 3, and 4, respectively. The UV absorption bands of NiL_i⁺ are attributed to CTTS transitions. The kinetics of reduction of Co(NH₃)₆³⁺, Ru(NH₃)₆³⁺, O₂, and N₂O by NiL_i⁺ are reported and discussed. The self-exchange rates of reaction between NiL_i⁺ and NiL_i²⁺ were calculated by using the Marcus cross relation. The EPR spectra of NiL₂⁺ and NiL₄⁺ are reported. The complexation of NiL_i²⁺ by OH⁻ was studied. The results are discussed in detail. NiL₂⁺ and NiL₄⁺ are suggested as new, powerful, easily attainable single-electron-reducing agents that can be used over a wide pH range in aqueous solutions.

Introduction

We have recently observed that the reduction of the planar isomer of (*C-meso*-1,4,5,7,7,8,11,12,14,14-decamethyl-1,4,8,11-tetraazacyclotetradecane)nickel(II), NiL₄²⁺, yields the corresponding monovalent complex, which is surprisingly stable in aqueous solutions.² The kinetic stability of NiL₄⁺ in comparison to that of NiL₃⁺, L₃ ≡ *C-meso*-5,7,7,12,14,14-hexamethyl-1,4,8,11-tetraazacyclotetradecane, was attributed to two main factors; (a) The ligand loss reaction



is hindered or at least considerably slowed down by N-methylation. (b) The two-electron reduction of water



is endothermic for L = L₄ whereas it is exothermic for L = L₃.³ The differences in the redox potentials of NiL₄²⁺ and NiL₃²⁺ were attributed to the more hydrophobic nature of NiL₄²⁺ in comparison with that of NiL₃²⁺ and/or to the fact that the nickel-nitrogen bond length is larger in NiL₄²⁺.²

Due to the interest in the effect of macrocyclic ligands on the redox properties of transition-metal complexes in general and nickel complexes specifically,⁴⁻⁹ we decided to extend these studies.

In this report we analyze the effect of nitrogen and carbon methylation of (1,4,8,11-tetraazacyclotetradecane)nickel(II), NiL₁²⁺, on the redox couple NiL₂²⁺/NiL₁⁺ by comparing the chemical properties of NiL₁⁺, NiL₂⁺, NiL₃⁺, and NiL₄⁺ (L₂ = 1,4,8,11-tetramethyl-1,4,8,11-tetraazacyclotetradecane). In addition to the electrochemical properties and specific rates of redox reactions studied by pulse radiolysis also the visible spectra of NiL₂²⁺ and pK values for the reaction



are reported. The last two properties are used as indicators for the ligand field strength and for steric hindrance along the z axis in the four complexes studied.

Experimental Section

Materials. The complexes NiL₁(ClO₄)₂ and NiL₃(ClO₄)₂ were prepared from the free ligands and Ni(CH₃CO₂)₂ as earlier described.⁹ NiL₂(ClO₄)₂ and NiL₄(ClO₄)₂ were prepared by N-methylation of NiL₁(ClO₄)₂ and NiL₃(ClO₄)₂, respectively, with use of the method described by Barefield et al.,¹⁰ i.e. deprotonation by solid KOH and methylation by CH₃I in Me₂SO. The IR spectra of NiL₂(ClO₄)₂ and NiL₄(ClO₄)₂ in KBr pellets showed no bands due to N-H stretching, and the proton NMR spectra of these complexes were identical with those reported in the literature.¹⁰

All other materials were of AR grade and were used without further treatment. All solutions were prepared with use of heat-distilled water that was then passed through a Millipore setup, the final resistance being >10 MΩ.

Electrochemical Measurements. A three-electrode cell was used. Working electrodes were a dropping mercury electrode (DME) for polarograms, the Metrohm E 410 hanging-mercury-drop electrode

- (1) (a) Ben-Gurion University of the Negev. (b) Deceased, Aug 5th 1981. (c) Nuclear Research Centre Negev.
 (2) Jubran, N.; Ginzburg, G.; Cohen, H.; Meyerstein, D. *J. Chem. Soc., Chem. Commun.* **1982**, 517.
 (3) *E*⁰ for the couple NiL₃(H₂O)₂³⁺/NiL₃²⁺ was estimated as *E*⁰ = 0.93 V vs. SCE.⁴ As NiL₃(H₂O)₂³⁺ has a p*K*_a at 3.7,⁵ *E*⁰ is even lower in neutral solutions. We were unable to oxidize NiL₄²⁺ even by Br₂⁻². Furthermore, the data in this work suggest that *E*⁰_{NiL₄³⁺/NiL₄²⁺} > *E*⁰_{NiL₃³⁺/NiL₃²⁺}.
 (4) Zeigerson, E.; Ginzburg, G.; Kirshenbaum, L. J.; Meyerstein, D. *J. Electroanal. Chem. Interfacial Electrochem.* **1981**, *127*, 113.
 (5) Cohen, H.; Kirshenbaum, L. J.; Zeigerson, E.; Jaacobi, M.; Fuchs, E.; Ginzburg, G.; Meyerstein, D. *Inorg. Chem.* **1979**, *18*, 2763.
 (6) Lovecchio, F. V.; Gore, E. S.; Busch, D. H. *J. Am. Chem. Soc.* **1974**, *96*, 3109.

- (7) Busch, D. H.; Pillsbury, D. G.; Lovecchio, F. V.; Tait, A. M.; Hung, Y.; Jackels, S.; Rakowski, M. C.; Schammel, W. P.; Martin, L. Y. *ACS Symp. Ser.* **1977**, *No. 38*, 32.
 (8) Haines, R. I.; McAuley, A. *Coord. Chem. Rev.* **1981**, *39*, 77.
 (9) Zeigerson, E.; Bar, I.; Bernstein, J.; Kirshenbaum, L. J.; Meyerstein, D. *Inorg. Chem.* **1982**, *21*, 73.
 (10) Wagner, F.; Barefield, E. K. *Inorg. Chem.* **1976**, *15*, 408. Wagner, F.; Morella, M. T.; d'Annello, M. J.; Wang, A. H. J.; Barefield, E. K. *J. Am. Chem. Soc.* **1974**, *96*, 2625.

Table I. Properties of NiL_i Complexes

	$E^\circ_{\text{NiL}_i^{2+}/\text{NiL}_i^+}$, V vs. SCE	$\lambda_{\text{max}}(\text{NiL}_i^+)$		$\lambda_{\text{max}}(\text{NiL}_i^{2+})^a$		$\text{pK}_a([\text{NiL}_i(\text{H}_2\text{O})_2^{2+}]/[\text{H}_3\text{O}^+][\text{NiL}_i(\text{H}_2\text{O})(\text{OH})^+])$
		nm	cm^{-1}	nm	cm^{-1}	
L_1	-1.58	375	26 670	455	21 980	13.67 ^b
L_2	-1.15	353	28 340	492	20 320	11.94 ^b
L_3	-1.42	380	26 320	468	21 370	>14.5
L_4	-0.98	335	29 850	516	19 380	13.6

^a In CH_3NO_2 . ^b From ref 11.

(HMDE) for CV measurements, and a mercury pool for preparative electrolysis. The auxiliary electrode was a Pt wire, and a SCE was used as a reference electrode. The auxiliary and reference electrodes were placed in separate compartments of the cell. All potentials are given vs. SCE. Polarograms were recorded on a Metrohm E 261 Polarecord with a Metrohm E 446 potentiostatic interface. CV measurements were performed with a GBU Model 208 polarographic analyzer potentiostat and a Tacussel Model GSTP 2 wave generator. All solutions were deaerated by N_2 , previously bubbled through a VSO_4 solution in dilute H_2SO_4 over Zn amalgam followed by a washing bottle.

Pulse Radiolysis. Pulses (0.1–1.5 μs , 200 mA, 5 MeV electrons) from the linear accelerator at the Hebrew University of Jerusalem were used. The dose per pulse was 100–3000 rd. The methods of preparing the solutions and analysis of the results were identical with those earlier described in detail.⁵

Spectroscopic Measurements. The spectra of ML^{2+} as well as the pK_a of the axially bound water, reaction 3, were determined with a Bausch and Lomb Spectronic 2000 spectrophotometer.

EPR Measurements. A Varian Model E12 X-band spectrometer was used. Measurements at room temperature and 77 K were carried out.

Results and Discussion

Electrochemical Reduction of NiL^{2+} . First of all we determined the electrochemical properties of the divalent nickel complexes as the knowledge of the redox potentials for the $\text{NiL}^{2+}/\text{NiL}^+$ couples is essential for analyzing their chemical properties.

Polarograms of solutions containing the NiL^{2+} complexes indicated that NiL_2^{2+} and NiL_3^{2+} are reduced in reversible one-electron processes. (The number of electrons was determined by comparison with the current obtained in solutions containing Cd^{2+} .) Plots of $\log(i/i_d - i)$ vs. the potential are linear with slopes of 59 mV. The polarographic reduction of NiL_4^{2+} is also a single-electron process, but the shape of the wave indicates that the process is quasi-reversible. The reduction waves of NiL_2^{2+} are preceded by a small prewave attributed to adsorption. The reduction waves are all independent of the supporting electrolyte, NaClO_4 , NaCl , NaH_2PO_4 , or $\text{N}(\text{CH}_3)_4\text{Cl}$. The complex NiL_1^{2+} is not reduced polarographically in aqueous solutions even in solutions at pH 12.7, 0.1 M $\text{N}(\text{CH}_3)_4\text{Cl}$, where the hydrogen wave appears at -1.70 V vs. SCE.

Cyclic voltammetry on a HMDE indicated also that the NiL_i^{2+} , $i = 2-4$, complexes are reduced in neutral and alkaline aqueous solutions and that the lifetime of NiL_i^+ is long enough so that its oxidation is observed on the back scan; i.e. $t_{1/2} \geq 1$ min. Whereas the voltammograms of NiL_2^{2+} and NiL_3^{2+} are simple and indicate a reversible one-electron-redox process, that of NiL_4^{2+} is slightly more complicated (see Appendix), though it fits also a single-electron-redox reaction.²

Cyclic voltammetry of NiL_1^{2+} on a HMDE at slow scan rates shows no reduction wave; at most a shoulder on the water reduction wave is observed. However, when the scan rate is increased (Figure 1a), a reduction wave is observed with $E^\circ_{1/2} = -1.56$ V vs. Ag/AgCl (Figure 1a). From the relative heights of the reduction and oxidation waves it is clear that the lifetime of NiL_1^+ is only a few seconds. The redox potentials of the $\text{NiL}^{2+}/\text{NiL}^+$ couples thus determined are summed up in Table I.

Cyclic voltammograms of NiL_2^{2+} in alkaline solutions show two reduction waves and a single oxidation wave on the back scan, which coulometrically equals the sum of the two reduction waves (Figure 1b). The second wave is attributed to the formation of a hydroxo complex of the type $\text{NiL}_2(\text{H}_2\text{O})(\text{OH})^+$ or $\text{NiL}_2(\text{OH})_2$ or $\text{NiL}_2(\text{OH})^+$ in equilibrium with NiL_2^{2+} .¹¹

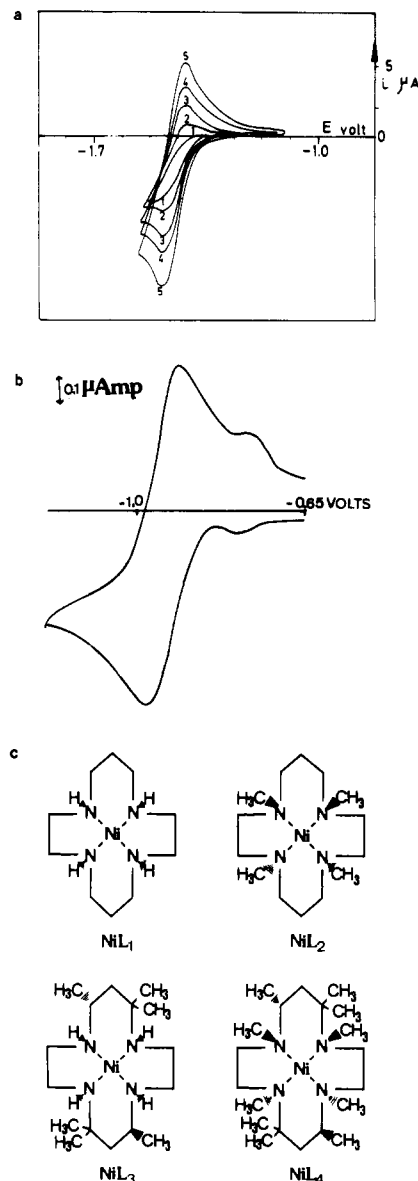
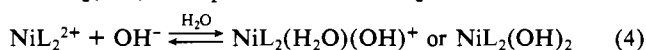


Figure 1. (a) Cyclic voltammograms of NiL_i^{2+} at different scan rates (5×10^{-3} M $\text{NiL}_i(\text{ClO}_4)_2$, 1 M NaClO_4 , pH 6.5, N_2 -saturated solution, on HMDE reference electrode Ag/AgCl): (1) 11 mV/s; (2) 22 mV/s; (3) 44 mV/s; (4) 66 mV/s; (5) 110 mV/s. (b) Cyclic voltammogram of NiL_2^{2+} in alkaline solution (1×10^{-3} M $\text{NiL}_2(\text{ClO}_4)_2$, 0.1 M Na_2HPO_4 , pH 12.7, on HMDE, N_2 -saturated solution), (c) Structure of NiL_i , $i = 1-4$.

The complex NiL_4^{2+} was reduced to completion with use of a mercury pool as the cathode at -1.2 V; coulometry proved that this is a single-electron process. The UV spectrum of the product, NiL_4^+ , was measured (Figure 2). Polarographic analysis during the preparative reduction showed a common oxidation-reduction wave. When oxygen was bubbled through the solution of NiL_4^+ , the spectral changes indicated that NiL_4^+ was quantitatively

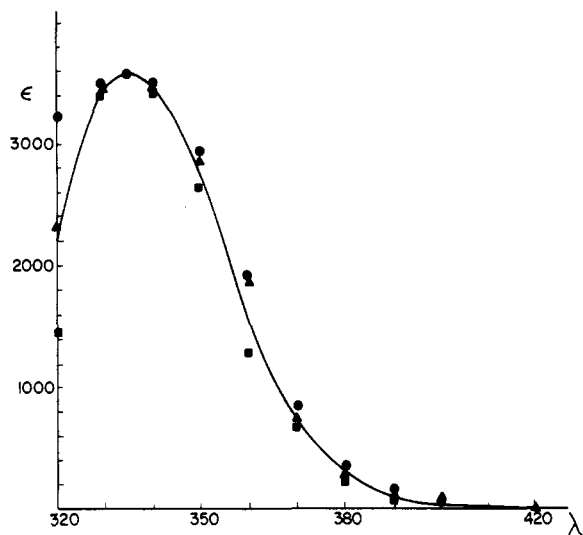


Figure 2. Absorption spectrum of NiL_4^+ (Ar-saturated solutions, 1×10^{-3} M $\text{NiL}_4(\text{ClO}_4)_2$, pH 7.0): (\blacktriangle) pulse radiolysis experiment (solution contained also 0.1 M HCO_2Na); (\bullet) ^{60}Co γ -source irradiation (solution contained also 0.1 M HCO_2Na , spectrum normalized at 335 nm relative to that of the pulse radiolysis experiment); (\blacksquare) preparative electrolysis (solution contained also 0.1 M $\text{N}(\text{CH}_3)_4\text{Cl}$, spectrum normalized at 335 nm relative to that of the pulse radiolysis experiment).

Table II. Electrocatalysis of Hydrogen Evolution by NiL_i^{2+} ^a

pH	E, V vs. SCE ^b			
	no additive	NiL_2^{2+}	NiL_3^{2+}	NiL_4^{2+}
1.5	-1.302	-1.300		-1.488
2.1	-1.346	-1.380		-1.546
3.5	-1.450	-1.506	-1.404	-1.576
4.0	-1.612	-1.526	-1.446	-1.588
4.6	-1.682	-1.550	-1.514	-1.622
5.3	-1.768	-1.578	-1.580	-1.650
6.2	-1.810	-1.648	-1.608	-1.672
7.2	-1.892	-1.680	-1.624	-1.646
12.7	-1.895	-1.892	-1.697	-1.880

^a All solutions contained 0.1 M NaH_2PO_4 . pH was adjusted with HClO_4 or NaOH as required. The concentration of NiL_i^{2+} is 1.0×10^{-3} M. ^b Potential at which a current of 28 μA at standard conditions is observed.

oxidized to NiL_4^{2+} . When a solution of NiL_4^+ is acidified by HClO_4 , a white air-sensitive precipitate is formed. Dissolution of this precipitate in air-free water yields a solution with a spectrum identical with that of NiL_4^+ , indicating that the precipitate is NiL_4ClO_4 . Addition of 0.1 M HCl to solutions containing NiL_4^+ causes the disappearance of the absorption band of NiL_4^+ without the appearance of a precipitate or of H_2 , as determined by gas chromatography. The nature of the latter process was not elucidated.

The complex NiL_2^{2+} was reduced preparatively in an analogous experiment at -1.3 V. The spectrum of NiL_2^+ consists of a strong absorption band, $\lambda_{\text{max}} = 353$ nm, identical with that observed in radiolytic studies (see below).

Electrocatalysis of Water Reduction. Tetraaza macrocyclic nickel complexes were shown to be electrocatalysts¹² and photoelectrocatalysts¹³ for the reduction of CO_2 . The formation of CO was always accompanied by the formation of H_2 .¹² We decided therefore to check whether the complexes studied in this work act as electrocatalysts for hydrogen evolution. Typical results are shown in Figure 3. The results clearly indicate that NiL_i^{2+} , $i = 2-4$, catalyze hydrogen evolution; i.e., the potential at which a given hydrogen evolution current is observed is less cathodic in the presence of the complexes. In Table II the results at several

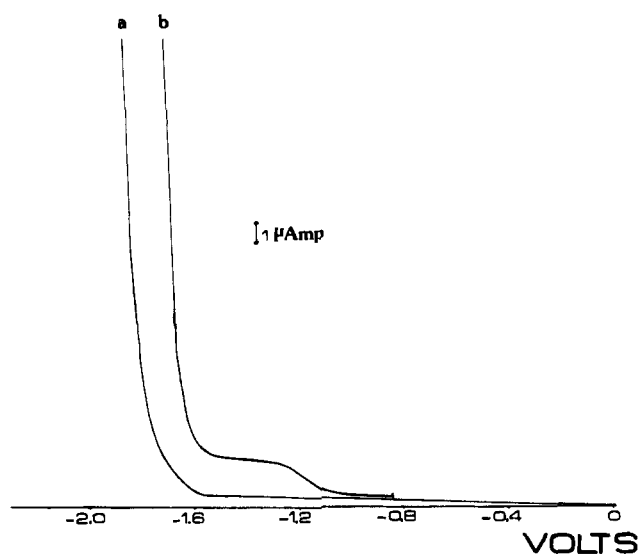
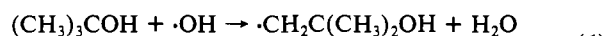
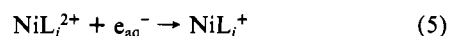


Figure 3. Polarograms on a DME (N_2 -saturated solutions): (a) 0.1 M NaH_2PO_4 , pH 7.2; (b) 1.0×10^{-3} M $\text{NiL}_2(\text{ClO}_4)_2$, 0.1 M NaH_2PO_4 , pH 7.2.

pHs are summed up. Also, the slopes of Tafel plots of the hydrogen evolution wave are decreased in the presence of the complexes; e.g., the Tafel slope in a solution containing 0.1 M phosphate at pH 6.2 is 160 mV and when 1×10^{-3} M NiL_2^{2+} is added is 80 mV. The results indicate that the catalysis is considerable, 100–270 mV, in slightly acidic and neutral solutions and decreases in alkaline solutions, and in acidic solutions the opposite effect is observed, probably due to adsorption of the complex on the mercury drop.

The results clearly indicate that the electrocatalysis does not stem from reaction 2 as the hydrogen evolution reaction does not start at the potentials where NiL_i^{2+} complexes are reduced. Thus, the catalytic effect seems to be due to a synergic effect of the complex and the mercury electrode at relatively large overpotentials.

Reduction of NiL_i^{2+} by e_{aq}^- and CO_2^- . Argon-saturated solutions containing 0.1 M *tert*-butyl alcohol and $(1-10) \times 10^{-5}$ M NiL_i^{2+} at pH 6.0 were irradiated by short electron pulses from the linear accelerator. Under these conditions reactions 5 and 6 are expected.¹⁴ The radical $\cdot\text{CH}_2\text{C}(\text{CH}_3)_2\text{OH}$ is a very weak



$$k = 5.2 \times 10^8 \text{ M}^{-1} \text{ s}^{-15}$$

reducing agent¹⁶ and is not expected to react with NiL_i^{2+} . The kinetics of disappearance of e_{aq}^- , observed at 600 nm, and appearance of a transient absorbing in the near-UV region were followed. From the dependence of these rates on $[\text{NiL}_i^{2+}]$ the specific rate constants of the reactions $e_{\text{aq}}^- + \text{NiL}_i^{2+}$ were determined and are summed up in Table III.

The spectra of NiL_i^+ thus formed were measured immediately after the reaction $e_{\text{aq}}^- + \text{NiL}_i^{2+} \rightarrow \text{NiL}_i^+$ was over λ_{max} (nm) (ϵ_{max} , $\text{M}^{-1} \text{ cm}^{-1}$) values are 375 (4500), 355 (3150), and 335 (3600) for NiL_1^+ , NiL_2^+ , and NiL_4^+ . (For NiL_3^+ $\lambda_{\text{max}} = 380$ nm and $\epsilon_{\text{max}} = 5150 \text{ M}^{-1} \text{ cm}^{-1}$ have been reported.¹⁷) The results indicated that NiL_1^+ and NiL_3^+ thus formed are short-lived. The latter observation was first noted for NiL_3^+ . This result is in full agreement with those reported by Tait et al.¹⁷ but contradicts the conclusions derived from the CV experiments.

(12) Fisher, B.; Eisenberg, R. *J. Am. Chem. Soc.* **1980**, *102*, 7361.
 (13) Bradley, M. G.; Tysak, T.; Graves, D. J.; Vlachopoulos, N. A. *J. Chem. Soc., Chem. Commun.* **1983**, 349.

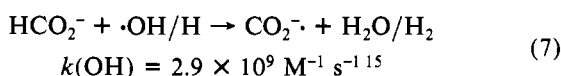
(14) Dorfman, L. M.; Matheson, M. S. "Pulse Radiolysis"; MIT Press: Cambridge, MA, 1969.
 (15) Farhatziz; Ross, A. B. *Natl. Stand. Ref. Data Ser. (U.S., Natl. Bur. Stand.)* **1977**, *NSRDS-NBS 59*.
 (16) Henglein, A. *Electroanal. Chem.* **1976**, *9*, 163.
 (17) Tait, A. M.; Hoffman, M. Z.; Hayon, E. *Inorg. Chem.* **1976**, *15*, 934.

Table III. Specific Rates of Reaction ($M^{-1} s^{-1}$) of NiL_i Complexes^a

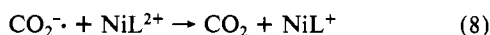
	L_1	L_2	L_3^b	L_4
$NiL_i^{2+} + e_{aq}^-$	3.8×10^{10}	1.2×10^{10}	5.6×10^{10}	8.7×10^{10}
$CO_2^{\cdot -}$	5.2×10^9	1.5×10^9	5.7×10^9	4×10^6
$NiL_i^+ + Ru(NH_3)_6^{3+}$	6.4×10^8	4.9×10^7	3.8×10^8	3.0×10^7
$Co(NH_3)_6^{3+}$	6.2×10^6	8.0×10^5	1.9×10^5	1.7×10^4
O_2	2.5×10^9	1.6×10^9	1.6×10^9	4×10^7
N_2O	3.2×10^7	8.3×10^2	3.9×10^7	<0.1
$NiL_i^{2+ c}$	1×10^{-3}	1×10^{-1}	3×10^{-2}	3
$Co(NH_3)_6^{3+ d}$	1.4×10^6	5.0×10^4	7.5×10^5	2.3×10^4
$Co(NH_3)_6^{3+ e}$	5.3×10^5	1.8×10^4	2.8×10^5	8.0×10^3

^a Measured by pulse radiolysis in neutral aqueous solutions. ^b From ref 19. ^c Calculated using the Marcus cross relation (see text). ^d Calculated from the Marcus cross relation using the calculated self-exchange rates between NiL_i^{2+} and NiL_i^+ and $1 \times 10^{-4} M^{-1} s^{-1}$ for the self-exchange rate between $Co(NH_3)_6^{3+}$ and $Co(NH_3)_6^{2+}$. ^e As for *d* but assuming a self-exchange rate of $1 \times 10^{-5} M^{-1} s^{-1}$ between $Co(NH_3)_6^{3+}$ and $Co(NH_3)_6^{2+}$.

We have therefore tried to produce the NiL_i^+ complexes under different conditions. Argon-saturated solutions containing 0.1 M HCO_2Na and $(1-10) \times 10^{-4} M NiL_i^{2+}$ at pH 6.0 were irradiated. Under these conditions reaction 6 is replaced by



The $CO_2^{\cdot -}$ radicals are very strong reducing agents, $E^\circ_{CO_2/CO_2^{\cdot -}} = -2.0 V$ vs. SCE,¹⁶ and are therefore expected to reduce the NiL_i^{2+} complexes:

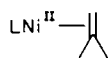


The rates of reaction 8 thus determined are summed up in Table III. The spectra of the monovalent complexes formed in reaction 8 are identical, within the experimental error limit, with those formed by the reaction of e_{aq}^- in the solutions containing *tert*-butyl alcohol. However, the lifetime of NiL_i^+ , $i = 1-3$, is considerably longer in solutions containing formate instead of *tert*-butyl alcohol. Thus, for example, at pH 6.0 $t_{1/2}$ is ca. 1 and 30 min for NiL_3^+ and NiL_2^+ , respectively, and at pH 5.0 ca. 2 s for both NiL_1^+ and NiL_3^+ .

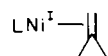
The stability of NiL_2^+ is higher in alkaline solutions; e.g., at pH 12.0 in formate solutions $t_{1/2}(NiL_2^+) \geq 3 h$. The results are in full agreement with those expected from the CV experiments and suggest that the mechanism of decomposition in the *tert*-butyl alcohol containing solutions is different. It is tempting to suggest that the sequence of reactions observed by Tait et al.¹⁷ and by us in the *tert*-butyl alcohol solutions involve reactions of the type



with or without the possible observation of transients of the type¹⁸



If excess NiL^+ remains in the solution after reaction 9 is over, which is plausible as NiL^+ and $\cdot CH_2C(CH_3)_2OH$ are formed in similar yields and the latter decomposes also via dimerization, then also the formation of



is probable.²⁰ Analogous reactions with $\cdot CH_2C(CH_3)_2OH$ and ethylene were observed for Ni^+_{aq} ^{20,21} and other low-valent tran-

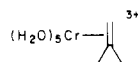
sition-metal complexes.²² The observation that NiL_4^+ is stable even in solutions containing *tert*-butyl alcohol suggests that reaction 9 is slow for NiL_4^+ , probably due to steric hindrance by the crowded ligand.

Kinetics of Reduction by NiL^+ . In order to study the effect of the change in the nature of L ligands on the reactivity of NiL^+ as a reductant, their reactions with $Ru(NH_3)_6^{3+}$, $Co(NH_3)_6^{3+}$, O_2 , and N_2O were studied. The kinetic results obtained in pulse radiolysis experiments are summed up in Table III. The reductions of $Co(NH_3)_6^{3+}$ and $Ru(NH_3)_6^{3+}$ by NiL_i^+ clearly proceed via the outer-sphere mechanism. The rates of reduction of $Ru(NH_3)_6^{3+}$ are always higher than those of $Co(NH_3)_6^{3+}$, as expected. For $Ru(NH_3)_6^{3+}$ the rates increase with the redox potential of NiL_i^+ (Table I). From the specific rates of reduction of $Ru(NH_3)_6^{3+}$, the redox potential of the NiL_i^+/NiL_i^{2+} and $Ru(NH_3)_6^{2+}/Ru(NH_3)_6^{3+}$ couples, and the specific rate of self-exchange of the latter couple the specific rates of the self-exchange reaction



can be calculated by using the Marcus cross relation.²³ (For the calculation it is assumed that even the reaction $NiL_1^+ + Ru(NH_3)_6^{3+}$ is considerably slower than the diffusion-controlled limit.) The results thus obtained are summed up in Table III. These results suggest that the rate of the self-exchange reaction, reaction 11, increases upon methylation of the ligand, the effect being larger for N-methylation than for C-methylation. It is tempting to suggest that methylation of the ligand decreases the hydrophilic nature of the complexes and thus decreases the outer-sphere rearrangement energy required for the self-exchange reaction. It should be noted that as the size of the cavity in the ligands L_i does not depend on the oxidation state of the central cation, a large fraction of the rearrangement energy it caused by the outer-sphere hydration shells. It is of interest to note that $k(Ni^+_{aq} + Ru(NH_3)_6^{3+}) = 4.0 \times 10^8 M^{-1} s^{-1 11}$ is similar to the rate of reaction of NiL_3^+ with $Ru(NH_3)_6^{3+}$; however, as $E^\circ_{Ni^+_{aq}/Ni^{2+}_{aq}}$ and k_{11} for Ni^+_{aq} are not known, a detailed comparison is impossible. We also note that the specific rate for the self-exchange of the NiL_i^{3+}/NiL_i^{2+} is considerably higher²⁵ than that of NiL_i^{2+}/NiL_i^+ . Using the calculated self-exchange rates of NiL_i^{2+} and NiL_i^+ , we calculated the expected rates of reaction of NiL_i^+ with $Co(NH_3)_6^{3+}$. A reasonable agreement with experiment is obtained if one assumes that the self-exchange rate for the $Co(NH_3)_6^{3+}/Co(NH_3)_6^{2+}$ couple is between 1×10^{-4} and $1 \times 10^{-5} M^{-1} s^{-1}$ (Table III). The latter values are higher than those commonly accepted but approach those recently suggested.²⁶

(18) It has been recently shown that



is the relatively long-lived intermediate in the OH^- elimination reaction from $(H_2O)_5CrCH_2C(CH_3)_2OH^{2+}$, and not the transients earlier suggested.¹⁹

(19) Cohen, H.; Shusterman, A.; Meyerstein, D.; Weiss, M. *J. Am. Chem. Soc.* **1984**, *106*, 1876.

(20) Kelm, M.; Lilie, J.; Henglein, A.; Janata, E. *J. Phys. Chem.* **1974**, *78*, 882.

(21) Freiberg, M.; Meyerstein, D. *J. Chem. Soc., Faraday Trans. 1* **1977**, *73*, 622.

(22) See, for example: Meyerstein, D. *Acc. Chem. Res.* **1978**, *11*, 43 and references therein.

(23) Marcus, R. A. *Annu. Rev. Phys. Chem.* **1964**, *15*, 155.

(24) Navon, G.; Meyerstein, D. *J. Phys. Chem.* **1970**, *74*, 4067.

(25) McAuley, A.; Macartney, D. H.; Oswald, T. *J. Chem. Soc., Chem. Commun.* **1982**, 274. Macartney, D. H.; McAuley, A. *Can. J. Chem.* **1983**, *61*, 103.

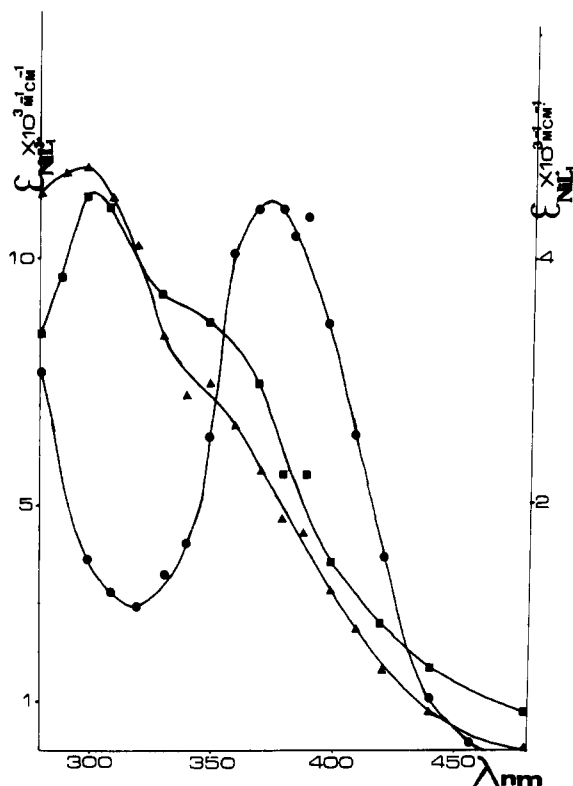
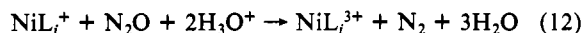
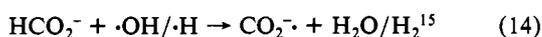


Figure 4. Spectra of transients observed in pulse radiolytic experiments in solutions of NiL_1^{2+} : (●) 2×10^{-4} M $\text{NiL}_1(\text{ClO}_4)_2$, 0.1 M HCO_2Na , pH 6.0, Ar-saturated solutions measured 20 μs after the pulse (scale on right); (■) 4×10^{-4} M $\text{NiL}_1(\text{ClO}_4)_2$, 0.1 M HCO_2Na , pH 6.0, N_2O -saturated solutions measured 40 μs after the pulse (scale on left); (▲) 4×10^{-4} M $\text{NiL}_1(\text{ClO}_4)_2$, 0.1 M KBr , pH 6.0, N_2O -saturated solutions measured 40 μs after the pulse (scale on left).

The mechanism of reaction of NiL_3^+ with N_2O was discussed by Tait et al.¹⁷ The atom-transfer mechanism

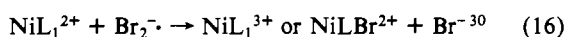
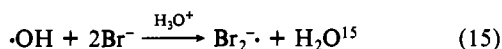


was proposed, in parallel with CoL_i^{+27} and $\text{Ni}^+_{\text{aq}}^{28}$ reactions, but as NiL_3^{3+} was not directly observed, the single-electron transfer via the outer-sphere mechanism was not ruled out.¹⁷ We measured the spectrum of the product of this reaction in N_2O -saturated solutions containing 4×10^{-4} M NiL_1^{2+} and 0.1 M HCO_2Na at pH 6.0; the results are presented in Figure 4. In these solutions all the primary radicals are converted into $\text{CO}_2^{\cdot-}$ via the reactions¹⁴



The $\text{CO}_2^{\cdot-}$ radicals reduce NiL_1^{2+} to yield NiL_1^+ via reaction 8 (Table III), and NiL_1^+ reacts with N_2O (Table III).

The spectrum of the product is very similar to that of NiL_1^{3+} or $\text{NiL}_1\text{Br}^{2+29}$ formed in N_2O -saturated solutions containing 4×10^{-4} M NiL_1^{2+} , and 0.1 M KBr at pH 6.0 (Figure 4). Under these conditions reaction 13 is followed by



(26) Geselowitz, D.; Taube, H. *Adv. Inorg. Bioinorg. Mech.* **1982**, *1*, 391.

(27) Tait, A. M.; Hoffman, M. Z.; Hayon, E. *J. Am. Chem. Soc.* **1976**, *98*, 86.

(28) Buxton, G. V.; Sellers, R. M.; McCracken, D. R. *J. Chem. Soc., Faraday Trans. 1* **1976**, *72*, 1464.

(29) Bromide and formate might ligate to $\text{NiL}_1(\text{H}_2\text{O})_2^{3+}$ in analogy to other anions with trivalent nickel complexes.⁹

(30) Jaacobi, M.; Meyerstein, D.; Lillie, J. *Inorg. Chem.* **1979**, *18*, 429.

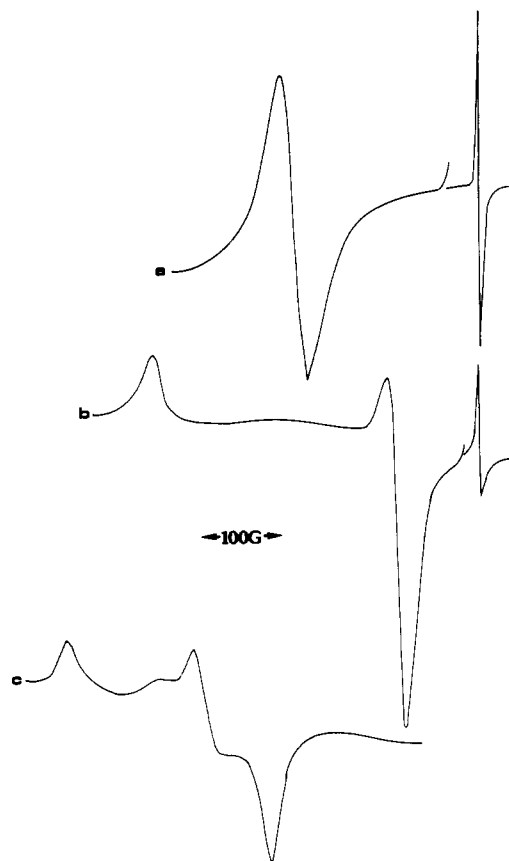
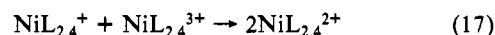


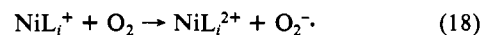
Figure 5. EPR spectra of NiL_4^+ : (a) 2×10^{-3} M $\text{NiL}_4(\text{ClO}_4)_2$, 1 M $(\text{CH}_3)_3\text{COH}$, pH 6.0, Ar-saturated solutions irradiated in the ^{60}Co γ -source, total dose 90000 rd, room temperature, reference DPPH; (b) same as (a) but 77 K; (c) 1×10^{-3} M $\text{NiL}_4(\text{ClO}_4)_2$, 0.1 M HCO_2Na , pH 5.5, Ar-saturated solutions, total dose 60000 rd, 77 K.

The similarity of the spectrum obtained in the formate solutions to that obtained in the bromide solutions indicates that indeed eq 12 correctly describes the mechanism of reaction of NiL_1^+ with N_2O .²⁹ NiL_2^{3+} and NiL_4^{3+} were not observed as the products of the analogous reactions of NiL_2^+ and NiL_4^+ with N_2O . This result is not surprising as, due to the low rates of reaction (Table III), reaction 17³⁰



is expected to compete efficiently with reaction 12 and inhibit the accumulation of NiL_2^{3+} . The low specific rates of reaction of NiL_2^+ and NiL_4^+ with N_2O probably stem from the fact that these reactions are thermodynamically considerably less favorable than the analogous reactions of NiL_1^+ and NiL_3^+ . Furthermore, the reactions might also be slowed down by steric hindrance toward attack along the z axis by the N -methyl groups. The latter effect contributes most probably in the NiL_4^+ system, as can be deduced from the low rate of the reaction of NiL_4^{2+} with $\text{CO}_2^{\cdot-}$ (Table III), though this is thermodynamically the most favorable reaction of $\text{CO}_2^{\cdot-}$ with NiL_i^{2+} . The latter result also suggests that the reactions of $\text{CO}_2^{\cdot-}$ with these complexes follow an inner-sphere mechanism, as k_{12} is highest for $\text{NiL}_4^{2+/+}$.

No NiL_i^{3+} complexes were observed as the final products of the reactions $\text{NiL}_i^+ + \text{O}_2$, and as, at least for $i = 1-3$, these are fast reactions, an electron-transfer mechanism

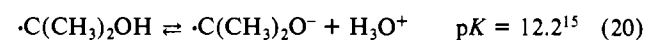
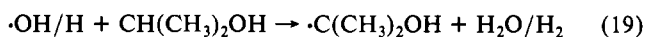


is indicated in accord with the conclusions of Tait et al. for the reaction $\text{NiL}_3^+ + \text{O}_2$.¹⁷

EPR of NiL_2^+ and NiL_4^+ . The EPR spectrum of NiL_4^+ formed by steady-state radiolysis of an Ar-saturated solution containing 1×10^{-3} M NiL_4^{2+} and 0.1 M $\text{C}(\text{CH}_3)_3\text{OH}$ at pH 5.7 is plotted in Figure 5. The results $g_{\text{av}} = 2.165$ at room temperature and $g_{\parallel} = 2.333$, $g_{\perp} = 2.069$, and $g_{\text{av}} = 2.157$ at 77 K are typical for

NiL_4^+ complexes.⁶ However, when NiL_4^+ is formed in Ar-saturated solutions containing 1×10^{-3} M NiL_4^{2+} and 0.1 M HCO_2Na at pH 5.7, the results at 77 K (Figure 5) indicate that the complex has lost its isotropic nature and an unisotropic spectrum typical for a d^9 metal with axial symmetry is observed with $g_1 = 2.261$, $g_2 = 2.136$, and $g_3 = 2.073$.³¹ When NiL_4^+ prepared in solutions containing $\text{C}(\text{CH}_3)_3\text{OH}$ is mixed 1:1 with a 0.2 M HCO_2Na solution, in the absence of air, and then frozen, the EPR spectrum retains its isotropic nature. We have no explanation for this phenomenon and plan to study it in detail. It is, however, tempting to speculate that the inner-sphere reduction of NiL_4^{2+} by CO_2^- ; (see above) requires some conformational isomerization, which does not occur in the outer-sphere reduction by e_{aq}^- . Such an isomerization might be similar to that induced by mercury and glassy carbon (see Appendix).

Similarly the EPR spectrum of NiL_2^+ formed by steady-state irradiation of an Ar-saturated solution containing 1×10^{-3} M NiL_2^{2+} and 0.1 M HCO_2Na at pH 7.5 gives $g_{\text{av}} = 2.162$ at room temperature and $g_1 = 2.270$, $g_2 = 2.137$, and $g_3 = 2.086$ at 77 K. NiL_2^+ cannot be formed in solutions containing $\text{C}(\text{CH}_3)_3\text{OH}$ (see above) but is formed in Ar-saturated solutions containing 1×10^{-3} M NiL_2^{2+} and 0.1 M $\text{CH}(\text{CH}_3)_2\text{OH}$ at pH 12.5. Under these conditions the radical $\cdot\text{C}(\text{CH}_3)_2\text{O}^-$, formed in the reactions



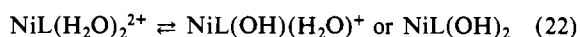
reduces NiL_2^{2+} . The EPR spectrum of NiL_2^+ in these solutions is isotropic; $g_{\text{av}} = 2.153$ at room temperature, and $g_{\parallel} = 2.313$, $g_{\perp} = 2.071$, and $g_{\text{av}} = 2.152$ at 77 K.

Spectra of NiL_i^{2+} in CH_3NO_2 . The absorption bands of these planar nickel complexes in the visible region originate from a $d_{xy} \rightarrow d_{x^2-y^2}$ transition. Therefore, the measurement of these spectra gives a direct determination of $10Dq_{xy}$. We chose nitromethane as the solvent for these measurements in order to minimize ligation along the z axis. The results are summed up in Table I; these results are in good agreement with those of Wagner et al.¹⁰

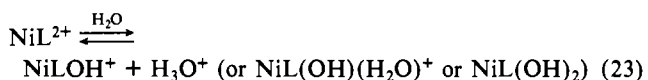
pK_a for Association of Hydroxides to NiL^{2+} . The tetraaza macrocyclic complexes of nickel in aqueous solutions are present in two forms: low-spin planar complexes and high-spin octahedral ones³³



In alkaline solutions the high-spin form exists as the hydroxo complex:



The hydroxo complexes might also appear as pentacoordinated high-spin complexes. The equilibrium constant K_{21} depends on the ligand field splitting caused by the ligand. Equilibrium 21 is clearly shifted to the right by increasing the hydroxide concentration. One also expects that the measured pK_a



will increase with the ligand field splitting in the complex. Indeed the reported pK_a 's for NiL_1^{2+} and NiL_2^{2+} ¹¹ are in accord with this expectation. We decided to measure the pK_a for NiL_3^{2+} and NiL_4^{2+} . For NiL_3^{2+} no evidence for reaction 23 was obtained up to 3 M KOH. For NiL_4^{2+} a dependence of the absorption spectrum on pH was observed (Figure 6), from which $pK_a = 13.6 \pm 0.15$ was calculated. When the KOH concentration is increased to 6 M, a green precipitate is formed. Solutions of it in neutral media have the absorption spectrum of NiL_4^{2+} .

The results thus indicate that $pK_a(\text{NiL}_3^{2+}) > pK_a(\text{NiL}_4^{2+})$, as expected from the ligand field splittings of these complexes as

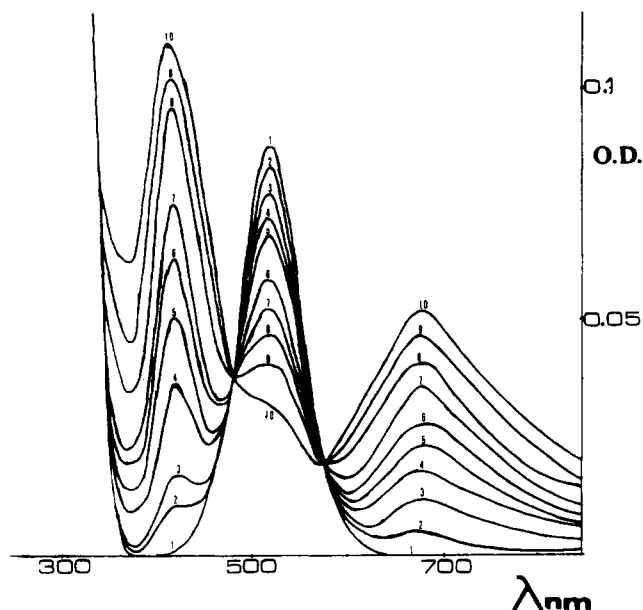


Figure 6. pH effect on the spectrum of NiL_3^{2+} (1.0×10^{-3} M $\text{NiL}_4(\text{ClO}_4)_2$): (1) pH 7.8; (2) pH 12.5; (3) pH 12.9; (4) pH 13.3; (5) pH 13.5; (6) pH 13.6; (7) pH 13.8; (8) 1 M KOH; (9) 2.5 M KOH; (10) 4 M KOH. An alkaline-stable glass electrode by Metrohm was used.

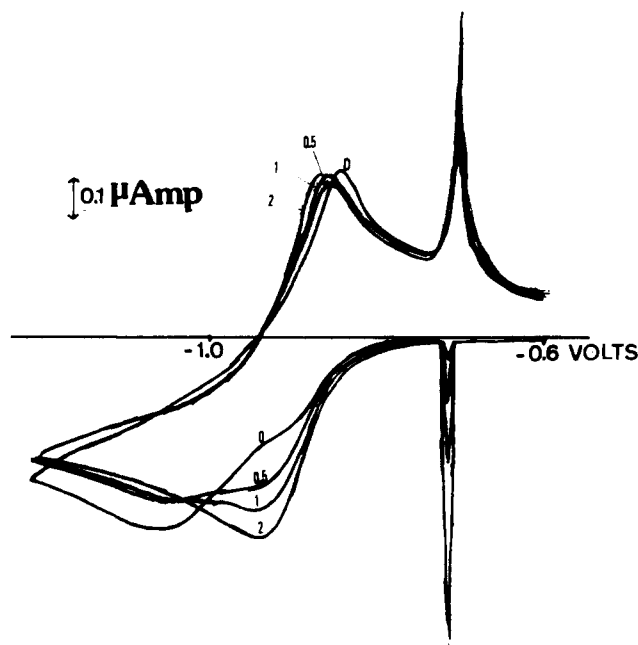


Figure 7. Time dependence of the CV of NiL_4^{2+} (N_2 -saturated solution, 3×10^{-4} M $\text{NiL}_4(\text{ClO}_4)_2$, 0.1 M $\text{N}(\text{CH}_3)_4\text{Cl}$, pH 6.0, scan rate 50 mV/s, on HMDE). The voltammograms were measured immediately after the drop was formed and 0.5, 1.0, and 2.0 min later.

determined spectrophotometrically (Table I). However, $pK_a(\text{NiL}_3^{2+}) > pK_a(\text{NiL}_1^{2+})$ and $pK_a(\text{NiL}_4^{2+}) > pK_a(\text{NiL}_2^{2+})$, though the opposite order is expected from the spectrophotometric measurements. The Ni-N bond distances increase along the series $\text{NiL}_1^{2+} < \text{NiL}_3^{2+} < \text{NiL}_2^{2+}$ ^{10,34,35} in agreement with the spectrophotometric results. Thus the increase in the pK_a caused by the six methyl substituents on L_3 is attributed to steric hindrance with the ligand bound along the z axis. It should be mentioned

(31) Similar spectra were observed for CO adducts of NiL_i^{2+} .³²

(32) Gagne, R. R.; Ingle, D. M. *Inorg. Chem.* **1981**, *20*, 420.

(33) Sabatini, L.; Fabbrizzi, L. *Inorg. Chem.* **1979**, *18*, 438 and references therein.

(34) Bosnich, B.; Mason, R.; Pauling, P. J.; Robertson, G. B.; Tobe, M. L. *J. Chem. Soc. Chem. Commun.* **1965**, 97. Ito, T.; Taniuchi, K. *Acta Crystallogr., Sect. B: Struct. Crystallogr. Cryst. Chem.* **1981**, *B37*, 88.

(35) The value for NiL_4^{2+} was not reported. The value for NiL_2^{2+} is only tentative,¹⁰ as the ligand, N_3^- , was bound to the z axis more strongly than the Cl^- used in the other studies.³⁴

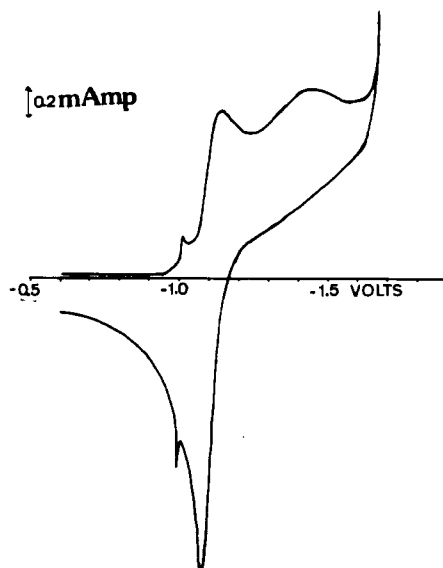


Figure 8. CV of NiL_4^{2+} after a long contact with a mercury pool (N_2 -saturated solution, 6×10^{-4} $\text{NiL}_4(\text{ClO}_4)_2$, 0.1 M NaH_2PO_4 , pH 7.0, scan rate 50 mV/s, on HMDE). The voltammograms were measured immediately after the drop was formed; the solution was mixed for 6 days over a mercury pool.

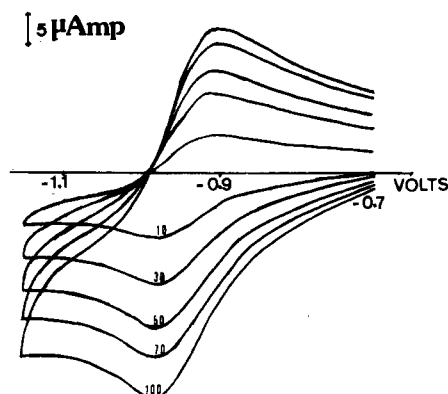


Figure 9. CV of NiL_4^{2+} on a glassy-carbon cathode (N_2 -saturated solution, 6×10^{-4} M $\text{NiL}_4(\text{ClO}_4)_2$, 0.1 M NaH_2PO_4 , pH 7.0). The numbers on the curves are the scan rates in mV/s.

that this is a somewhat surprising conclusion as sulfate and phosphate give stable complexes with NiL_3^{3+} .⁹ However, it seems that the effect of the decrease in the ligand field splitting in NiL_4^{2+} is larger than that of the increased steric hindrance as compared to the situation for NiL_3^{2+} .

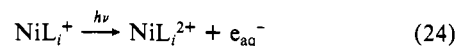
Concluding Remarks

The results support our expectation that methyl substituents bound to the nitrogens of 1,4,8,11-tetraazacyclotetradecane slow down the rate of the ligand-exchange reaction (1). This occurs though the cavity size of the ligand is increased,^{34,35} a fact that should accelerate the ligand loss reaction.³⁶

The dependence of the redox potentials of $\text{NiL}_i^{2+}/\text{NiL}_i^+$ on methylation (Table I) indicates that the major factor affecting the redox potential is the strength of the interaction between the central nickel ion and L_i . This conclusion is based on the correlation between the redox potentials and $10Dq_{xy}$ for NiL_i^{2+} as determined spectrophotometrically. This conclusion is in agreement with earlier reports.^{6,7} The results do not corroborate our earlier suggestion that the redox potential is strongly affected by the hydrophobicity introduced by the methyl substituents,² though

probably this effect has some contribution to the results.

When the maxima of the absorption bands of NiL_i^+ , $i = 2-4$, are plotted vs. the redox potentials, $E^\circ_{\text{NiL}_i^{2+}/\text{NiL}_i^+}$, a straight line is obtained. The slope of this line, when expressed in the correct energy unit, is 1. This observation suggests that the electronic transition occurring is a charge transfer to solvent transition:



The result for NiL_1^+ (Table I) strongly deviates from this correlation. It is plausible that this deviation is due to the difference in the structures of the outer-sphere hydration shell between ML_1^+ , which has no methyl substituents, and the methylated complexes.

Finally we would like to reemphasize that the results reported here indicate that NiL_2^+ and NiL_4^+ are powerful single-electron-reducing agents. These reducing agents can be easily prepared by electrochemical methods. They can be used over a wide pH range where few other strong reductants are available.

Acknowledgment. We are indebted to Professor Daryle Busch for helpful discussions. This study was supported in part by the Israel-U.S. Binational Science Foundation (BSF), Jerusalem, Israel, and by the PEF, Israel Endowment Funds, Inc., New York, NY.

Appendix. "Isomerization" of NiL_4^{2+}

Cyclic voltammograms of NiL_4^{2+} using a HMDE as the working electrode indicate that the shape of the voltammogram depends on the time elapsed from the formation of the mercury drop till the CV experiment was initiated (Figure 7). This time dependence is independent of the supporting electrolyte used, NaClO_4 , Na_2SO_4 , or $[\text{N}(\text{CH}_3)_4]\text{Cl}$. However, increasing the temperature of the solution or raising the pH to 12 accelerates the process, causing the change in the form of the voltammogram. On the other hand, increasing the concentration of NiL_4^{2+} from 3×10^{-4} to 1.0×10^{-3} M slows down the process so that the change equivalent to that observed in Figure 7 takes 8 min instead of 2 min. All these results suggest that the mercury surface causes some type of isomerization of NiL_4^{2+} . To check this point, a solution of 6×10^{-4} M NiL_2^{2+} in 0.1 M phosphate buffer at pH 7.0 was stirred mechanically over a mercury pool for 6 days. The CV on a fresh drop is plotted in Figure 8. This CV is identical with that observed in the same solution before stirring over the mercury pool, 7 min after the formation of the drop. This result supports the idea of isomerization of the complex on the mercury surface. However, the UV-vis spectra of NiL_4^{2+} prior to and after stirring over the mercury pool are identical.

Stirring the solution over a platinum gauze had no effect on the shape of the CV on a fresh HMDE, indicating that platinum does not induce the isomerization reaction. On the other hand, cyclic voltammograms on a glassy-carbon electrode, even immediately after immersion in the solution, indicate a reversible single-electron-redox process (Figure 9). This result suggests that the rate of "isomerization" on the glassy-carbon surface is fast.

The ligand in NiL_4^{2+} cannot isomerize without bond breaking, which clearly does not happen under the mild conditions described. Thus we suggest that the process observed is due to some change in the conformation of the complex induced by the mercury or carbon surfaces. The ligand in this complex has a relatively large strain energy due to the 10 methyl groups. It is conceivable that the complex crystallizes in a configuration slightly different from that most stable in aqueous solutions. The mercury or carbon surfaces might act as catalysts to this small configurational isomerization. Even larger isomerizations of NiL_2^{2+} were recently reported to be relatively fast in several solvents.³⁷

It should be noted that the CV after isomerization is that of a reversible one-electron-redox process. The redox potential (Table I) was measured after isomerization. The small prewave observed

(36) Freiberg, M.; Meyerstein, D.; Yamamoto, Y. *J. Chem. Soc., Dalton Trans.* 1982, 1137.

(37) Moore, P.; Sachinidies, J.; Willey, G. R. *J. Chem. Soc., Chem. Commun.* 1983, 522.

in Figure 8 is attributed to adsorption. It is of interest to note that also this wave is smaller after isomerization.

Registry No. NiL₁(ClO₄)₂, 57456-82-3; NiL₂(ClO₄)₂, 57427-14-2; NiL₃(ClO₄)₂, 57456-81-2; NiL₄(ClO₄)₂, 57427-09-5; NiL₁⁺, 93984-20-4;

NiL₂⁺, 59461-43-7; NiL₃⁺, 94061-35-5; NiL₄⁺, 84026-55-1; NiL₃-(H₂O)₂²⁺, 93923-56-9; NiL₄(H₂O)₂²⁺, 93984-21-5; Co(NH₃)₆³⁺, 14695-95-5; Ru(NH₃)₆³⁺, 18943-33-4; N₂O, 10024-97-2; CO₃²⁻, 85540-96-1; (CH₃)₃COH, 75-65-0; H₂O, 7732-18-5; H₂, 1333-74-0; O₂, 7782-44-7.

Contribution from the Department of Chemistry,
University of Kentucky, Lexington, Kentucky 40506-0055

Preparation and Absorption and Emission Spectra of *cis*-Bis(2-hydroxy-6-methylpyridinato)bis(triethylphosphine)dichlorodimolybdenum(II)

PHILLIP E. FANWICK

Received June 26, 1984

The quadruply bonded dimer *cis*-Mo₂(mhp)₂Cl₂(PEt₃)₂ was prepared by the reaction of a stoichiometric amount of SiCl(CH₃)₃ with Mo₂(mhp)₄ in the presence of the phosphine. The compound crystallized in a triclinic cell (space group *P* $\bar{1}$) with cell constants *a* = 9.953 (1) Å, *b* = 11.149 (1) Å, *c* = 15.602 (2) Å, α = 92.35 (1)°, β = 93.45 (1)°, γ = 115.51 (1)°, and *Z* = 2. Six transitions were observed in the solution spectrum, and the lowest energy band at 540 nm was assigned as $\delta \rightarrow \delta^*$. At 5 K, the 0-0 transition and seven vibronic origins were observed. All the progressions observed were based on the Mo-Mo stretching frequency, which was 370 (12) cm⁻¹ in the excited state. Strong fluorescence at 600 nm was observed from the $\delta^* \rightarrow \delta$ transition. The quantum yield was a function of wavelength varying from 0.24 at 540 nm to 0.09 at 305 nm. The fluorescence lifetime was 33.8 ns.

Introduction

Over the past several years there has been an extensive study of the electronic spectroscopy of the quadruply bonded dimers.^{1,2} These systems have been of interest because their bond orders are unusual and also because their spectra are very amenable to study by a variety of techniques. The absorption spectroscopy of the molybdenum dimers has been thoroughly examined, and the lowest energy transition has been assigned as $\delta \rightarrow \delta^*$. Of late, there has been much interest in the emission spectra of these dimers because there has been some question as to the assignment. In studies on Re₂Cl₈²⁻ and Mo₂Cl₈⁴⁻ it was found that the 0-0 transitions of the absorption and emission bands did not overlap.³ This was attributed to a change in the excited-state geometry from the rigorously eclipsed geometry found in the ground state to a staggered conformation. It was later found that this change in geometry did not occur in Mo₂Cl₄(PBU₃)₄ because of the bulky phosphines.^{4,5} In this case, the 0-0 bands nearly coincided. These studies have been pursued further and applied to a series of dimers of the form Mo₂Cl₄(PR₃)₄ (R = Me, Et, Pr, Bu).⁶ In all cases, the 0-0 bands are identical for the absorption and emission. However, the lifetime quantum yield and band shape are dependent on the halide and the R group of the phosphine.

So far, the only dimers to have their photochemistry fully studied have not had bridging ligands. The emission spectra of Mo₂(mhp)₄ and Mo₂(chp)₄ (mhp = 2-hydroxy-6-methylpyridine anion; chp = 2-hydroxy-6-chloropyridine anion) in inert matrices have been reported.⁷ However, no lifetime or quantum yields were given. In this paper, the synthesis, crystal structure, and absorption and emission spectra are reported for *cis*-Mo₂-(mhp)₂Cl₂(PEt₃)₂. In addition, the lifetime and quantum yields have been determined and are the first data for a bridged quadruply bonded dimer.

Experimental Section

Preparation of *cis*-Mo₂(mhp)₂Cl₂(PEt₃)₂. Typically 1.0 g (1.6 mmol) of Mo₂(mhp)₄ prepared by the standard method⁸ was refluxed in 50 mL

of THF with 0.348 g (3.2 mmol) of chlorotrimethylsilane and 0.40 g (3.4 mmol) of triethylphosphine for 3-4 h. The resulting dark red solution was evaporated to dryness, and the residue was chromatographed twice on activated silica gel, with cyclohexane as the solvent. The isolated yield was 60%. The resulting *cis*-Mo₂(mhp)₂Cl₂(PEt₃)₂ is bright red and is soluble in nearly all organic solvents. The solid appears to be indefinitely stable in air while solutions decompose only slowly. This same dimer can be prepared by the reaction of Mo₂Cl₄(PEt₃)₄ with mhp in the presence of NEt₂H.

Spectroscopy. The solution spectrum was recorded on a Beckman Model 26 UV-visible spectrophotometer and manually digitalized. The single-crystal spectrum was recorded on a Cary 17-D spectrophotometer interfaced by Varian Instruments to an Apple Computer. Two Ealing Optics Glan-Thompson prism polarizers were used, one located behind the sample and one in the reference beam. A Janis Super-Varitemp cryostat was used for the low-temperature studies. Deconvolution of the spectra was done by the method of damped least squares.⁹ Mass spectra were recorded on a Vacuum Generators ZAB-2F double-focusing spectrometer. Emission spectra were recorded on a Spex Fluorolog 2 fluorescence spectrophotometer. All solution studies were done with cyclohexane as the solvent. Excitation spectra were corrected for wavelength dependence with use of a Rhodamine B quantum counter. Spectra were obtained at 77 K by immersing a quartz sample tube into a partially silvered quartz dewar filled with liquid nitrogen. Spectra were obtained as methylcyclohexane glasses. A Photochemical Research Associates fluorescence lifetime instrument was used to determine the lifetime. The excitation source was a nitrogen flash lamp operated at 380.5 nm.

Crystallography. Crystals of *cis*-Mo₂(mhp)₂Cl₂(PEt₃)₂ were obtained by evaporation of acetone solutions. The crystal used was a kite shaped plate with dimensions 0.30 × 0.18 × 0.05 mm. The large, well-developed face was the (001) face. The crystal was mounted on a glass fiber with epoxy cement. Indexing and data collection were done by using an Enraf-Nonius CAD-4 automatic diffractometer. The cell constants determined from the least-squares fit of 25 reflections with 24° < 2θ < 35° were *a* = 9.953 (1) Å, *b* = 11.149 (1) Å, *c* = 15.602 (2) Å, α = 92.35 (1)°, β = 93.45 (1)°, γ = 115.51 (1)°, and *V* = 1555 Å³. For the formula Mo₂Cl₂P₂O₂N₂C₂₄H₄₂ the calculated molecular weight is 715.32 and for *Z* = 2 the calculated density is 1.53 g/cm³. Data were collected at 22 °C by using the θ -2 θ scan technique and graphite-monochromated Mo K α radiation. The details of data collection and structure refinement have been reported previously.¹⁰ Of the 4062 unique data collected, only the 3098 data with *I* ≥ 3 σ (*I*) were used in the structure refinement. The absorption coefficient was 10.9 cm⁻¹ and an empirical absorption correction was applied.¹¹

Refinement was begun and ultimately converged in the space group *P* $\bar{1}$. The positions of the molybdenum atoms were determined from a

- (1) Cotton, F. A.; Walton, R. A. "Multiple Bonds Between Metal Atoms"; Wiley: New York, 1982.
- (2) Trogler, W. C.; Gray, H. B. *Acc. Chem. Res.* **1978**, *11*, 232-239.
- (3) Trogler, W. C.; Solomon, E. I.; Gray, H. B. *Inorg. Chem.* **1977**, *16*, 3031-3033.
- (4) Trogler, W. C.; Gray, H. B. *Nouv. J. Chim.* **1977**, *1*, 475-476.
- (5) Miskowski, V. M.; Goldbeck, R. A.; Kliger, D. S.; Gray, H. B. *Inorg. Chem.* **1979**, *18*, 86-89.
- (6) Gray, H. B.; Hopkins, M. D. *J. Am. Chem. Soc.* **1984**, *106*, 2468-2469.
- (7) Manning, M. C.; Trogler, W. C. *J. Am. Chem. Soc.* **1983**, *105*, 5311-5320.
- (8) Cotton, F. A.; Fanwick, P. E.; Niswander, R. H.; Sekutowski, J. C. *J. Am. Chem. Soc.* **1978**, *100*, 4725-4732.

- (9) Papousek, D.; Pliva, J. *Collect. Czech. Chem. Commun.* **1965**, *30*, 3007-3015.
- (10) Fanwick, P. E.; Huckaby, J. L. *Inorg. Chem.* **1982**, *21*, 2067-2071.
- (11) Flack, H. D. *Acta Crystallogr., Sect. A* **1977**, *A33*, 890-898.